

# The Simple Geometry of Time: A Physical Record of Cosmic Metric Transformation

Alata Elatawneh

Alumni, Technical University of Munich (TUM), Germany

June 2026

## Abstract

We present a predictive, geometrically constrained cosmological architecture, designated the Unified Cosmic Kinematic (UCK) framework, derived from the foundational postulate that cosmic time is macroscopically identical to relational metric spatial expansion. The invariant comoving time derivative of this identity demonstrates that the unperturbed background expansion parameter is the analytical inverse of the cosmic epoch, yielding a global background baseline constant of  $70.85 \text{ km s}^{-1} \text{ Mpc}^{-1}$  when anchored to the empirically observed cosmic age of 13.8 Gyr. Although the baseline expansion model is geometrically deterministic, mapping observational signatures requires accounting for the interaction of matter and radiation within the spatial manifold via an effective field theory approach. This framework introduces four native tracking parameters calculated from first principles via the optimization of unbinned data streams, independent of external fluid-driven dark sector parameters. The statistical viability of this architecture is evaluated against five high-precision, unbinned astronomical data pipelines spanning late-universe standard candles, local velocity anomalies, localized mass-deflection geometries, the cosmic microwave background, and deep spectroscopic horizons. Our optimization routines address the persistent Hubble tension by demonstrating that regional gravitational density induces a localized clock-drag fraction that elevates the apparent local expansion rate via gravitational time dilation. This exact localized clock-drag metric reconciles weak-field gravitational limits, precisely mapping the mass-deflection profiles of strong gravitational lensing systems under pure baryonic constraints without invoking dark matter halos. Finally, coupling this expansion history to the primordial plasma sound horizon maps the early acoustic peaks with high statistical fidelity. The resulting high-redshift temporal elongation extends the available structural development timeline, thereby addressing the early mature galaxy chronological discrepancy across all targeted spectroscopic horizons.

## 1 Introduction

Modern precision cosmology faces critical empirical contradictions that challenge the foundational infrastructure of the standard model. The consensus model of cosmology, Lambda Cold Dark Matter ( $\Lambda$ CDM), which has been successful at tracing large-scale cosmic averages, operates primarily as a phenomenological description rather than a predictive, first-principles framework. It relies on a suite of free, adjustable parameters—including the modern Hubble expansion rate ( $H_0$ ), dark matter fractions ( $\Omega_{m,0}$ ), and dark energy coordinates—which must be continuously updated to accommodate evolving datasets. Concurrently, high-precision data from next-generation observatories have pushed these descriptive parametrizations to their mathematical limits, introducing structural tensions at opposite boundaries of the cosmic timeline [1–3].

The first of these challenges is the Hubble tension, a statistically significant discrepancy between the background and local calibrations of the universal expansion rate [2]. High-precision measurements of the early universe, captured by the Planck satellite via the cosmic microwave background (CMB) angular scale, calculate a global background value of  $H_0 = 67.4 \pm 0.5 \text{ km} \cdot \text{s}^{-1} \cdot \text{Mpc}^{-1}$  [1]. Conversely, direct late-universe calibrations using nearby Type Ia supernovae and Cepheid variables from the Supernovae and  $H_0$  for the Equation of State of Dark Energy (SH0ES) collaboration, alongside recent James Webb Space Telescope (JWST) cosmic distance ladders, consistently yield a significantly higher local expansion rate of  $H_0 = 73.0 \pm 1.0 \text{ km} \cdot \text{s}^{-1} \cdot \text{Mpc}^{-1}$  [2]. Because the statistical tension between these independent pipelines has exceeded the  $5\sigma$  significance threshold, the mismatch can no longer be readily attributed to instrumental systematics or local cosmic variance, signaling a potential breakdown in the standard geometric understanding of cosmic acceleration.

The second challenge is the high-redshift galaxy timeline problem, a severe chronological discrepancy that has emerged at extreme redshifts following recent deep-field spectroscopic observations. The JWST Advanced Deep Extragalactic Survey (JADES) collaboration and corresponding deep imaging campaigns have revealed an abundance of massive, highly evolved, metallicity enriched galaxies thriving at redshifts  $z > 10$ , including the current distance record holder, JADES-GS-z14-0 at  $z = 14.32$  [3]. Standard flat- $\Lambda$ CDM equations under the consensus Planck 2018 baseline restrict the total available age of the universe at  $z = 14.32$  to 287.3 Myr. Because the nucleosynthesis of heavy elements and the gravitational assembly of dense galactic cores typically require extended thermodynamic timescales, the existence of these mature early structures challenges established stellar population constraints and dark matter halo growth models.

The foundational thesis of this work is predicated upon a strict relational identity between cosmic duration and metric expansion: we hypothesize that the macroscopic progression of cosmic time is fundamentally identical to the isotropic expansion of the spatial manifold at the invariant speed of light,  $c$ . By treating temporal duration not as an independent, background-dependent coordinate parameter but as the direct physical consequence of metric volume generation, this postulate establishes a rigid causal coupling across cosmological scales. Mathematically, this identity locks the scale factor  $a(T)$  to the elapsed cosmic calendar via the boundary relation  $a(T) = cT/\mathcal{R}_0$ , thereby eliminating independent gauge freedom from the global expansion law. Consequently, the unperturbed background expansion rate reduces to an elegant geometric necessity—the exact mathematical inverse of the global cosmic epoch,  $H_{\text{global}} = 1/T$ —offering a highly constrained, parameter-free baseline that can be directly verified or falsified by modern observational datasets.

It is critical to clarify the epistemological status of the quantitative baseline used in this study. Although the mathematical architecture of the UCK framework operates via this rigid geometric identity ( $H_{\text{global}} = 1/T$ ), its numerical evaluation at the current epoch necessitates the integration of a boundary condition derived from modern observational astronomy. We explicitly adopt the consensus value for the elapsed age of the universe,  $T_0 \approx 13.8 \text{ Gyr}$  (where  $1 \text{ Gyr} \equiv 10^9 \text{ years}$ ), established via high-precision cosmic chronometers, white dwarf cooling sequences, and globular cluster baryonic turn-off points [1]. We treat this temporal duration as an empirically constrained external anchor rather than an unperturbed deduction from a priori first principles.

By inserting this observational input into the derived inverse-expansion formulation, the framework yields a definitive global background baseline of  $H_{0,\text{theoretical}} \equiv 70.8545 \text{ km} \cdot \text{s}^{-1} \cdot \text{Mpc}^{-1}$ . Therefore, this value should be understood as a structural geometric projection of the observed modern temporal horizon, functioning as an analytical midpoint that naturally straddles the divergent local and deep-space expansion rates currently defining the Hubble tension.

Crucially, mapping observational data onto this global background canvas requires accounting for localized mass density distributions and high-energy boundary shifts. This mapping introduces four foundational tracking variables: the late-universe metric path resistance  $\beta$ , the localized

gravitational clock-drag fraction  $\delta$  (which modulates both large-scale velocity fields and localized mass-deflection geometries), and the early-universe quantum-scaling coefficients  $\alpha$  and  $\gamma$ . We emphasize that these four variables are entirely native to the UCK architecture, derived through independent algorithmic optimizations of raw, unbinned astronomical data streams. They do not retro-fit or translate any pre-existing fluid-density parameters ( $\Omega_m, \Omega_\Lambda, \Omega_b$ ), inflationary indices, or phenomenological variables from the standard model. Instead, they represent an isolated, self-contained mathematical suite derived directly from the intrinsic geometric equations of the framework.

The description of the early universe in standard cosmology remains mathematically incomplete. At time  $T \rightarrow 0$ , classical general relativity breaks down into an unphysical singularity characterized by infinite curvature, infinite density, and the absolute collapse of spacetime geometry. To circumvent early uniformity paradoxes, modern theory relies on cosmic inflation—a hypothesized primordial scalar field that assumes space expanded exponentially faster than light immediately following the initial singularity [4]. In this study, we show that these multi- $\sigma$  crises are not independent anomalies requiring distinct, ad hoc dark fluids, but are resolved by shifting cosmology from descriptive parametrizations to an absolute relational scale factor. We present a constrained architecture that does not rely on arbitrary parameter adjustments, but is anchored by an empirically calibrated baseline, systematically addressing the primary contradictions in modern astronomy.

The remainder of this paper is organized as follows. In Section 2, we establish the mathematical foundations of the UCK architecture, derive the velocity-inverse law of relational time from first principles, and execute a single-step global baseline boundary calculation. In Section 3, we detail our unbinned observational data methodology and empirical validation, subjecting the framework sequentially to the 1,701 unbinned Pantheon+ supernova dataset (Experiment 1), local baseline flow constraints (Experiment 2), the Planck 2018 high-multipole acoustic matrix (Experiment 3), the JWST JADES spectroscopic horizon (Experiment 4), and precise strong gravitational lensing mass-deflection profiles (Experiment 5). In Section 4, we present a rigorous comparative discussion, evaluating the UCK metric directly against standard dark-energy frameworks, spatial cosmic variance models, and alternative gravitational formulations. In Section 5, we present a comprehensive synthesis scorecard matrix and explicitly outline the framework’s limitations, theoretical justifications, and falsifiable observational predictions. Finally, in Section 6, we summarize our core cosmological conclusions and outline future research horizons.

## 2 Mathematical Foundations and Baseline Derivation

### 2.1 The Relational Scale Postulate: Relational Metric Growth and the Spacetime Line Element

We configure our cosmological framework by defining the forward progression of cosmic time ( $T$ ) as macroscopically identical to the relational metric expansion of space itself. The postulate that the macroscopic metric expansion of space proceeds fundamentally at the speed of light establishes a rigid causal constraint on the spacetime fabric. To formalize this geometric interaction under a smooth, isotropic, and homogeneous manifold, we map our relational scale factor directly onto a modified four-dimensional Friedmann-Lemaître-Robertson-Walker (FLRW) line element.

Let  $T$  denote the global background cosmic temporal coordinate mapping the cumulative chronological state of the cosmos. The universal background scale factor  $a(T)$  is locked to this time-line variable by the invariant vacuum speed of light  $c$  and an invariant relational spatial boundary

radius  $\mathcal{R}_0$ , which acts as a static infrared (IR) length scale of the global causal horizon:

$$a(T) = \frac{cT}{\mathcal{R}_0} \quad (1)$$

Unlike standard cosmological conventions, in which the modern scale factor is manually normalized to unity ( $a(T_0) \equiv 1$ ), the Unified Cosmic Kinematic (UCK) framework treats  $a(T)$  as a dynamically evolving dimensionless ratio. The parameter  $\mathcal{R}_0$  is strictly defined as a static, invariant fundamental constant of nature representing the core spatial length scale of the causal universe. Consequently, the value of  $a(T)$  at any given epoch—including our modern coordinate  $a(T_0)$ —is not artificially constrained but evaluates naturally to the scalar quantity dictated by the chronological progression of the cosmic calendar relative to this fixed infrared boundary.

By embedding this relational scale factor identity into the standard cosmological metric, we define the explicit invariant spacetime interval  $ds^2$  governing the global universal background as follows:

$$ds^2 = -c^2 dT^2 + [a(T)]^2 \left[ \frac{dr^2}{1 - kr^2} + r^2 d\theta^2 + r^2 \sin^2 \theta d\phi^2 \right] \quad (2)$$

Substituting Equation (1) into the spatial sector yields the explicit UCK background line element

$$ds^2 = -c^2 dT^2 + \left( \frac{cT}{\mathcal{R}_0} \right)^2 \left[ \frac{dr^2}{1 - kr^2} + r^2 d\Omega^2 \right] \quad (3)$$

where  $k \in \{-1, 0, 1\}$  represents the normalized spatial curvature index and  $d\Omega^2 \equiv d\theta^2 + \sin^2 \theta d\phi^2$  is the standard metric on a unit two-sphere.

This explicit metric configuration alters the structural interpretations found in standard general relativity. In standard cosmology, mass-energy distributions dynamically curve an independent, passive four-dimensional spacetime sheet via the Einstein field equations, allowing coordinate clocks to tick uniformly across an abstract background canvas. In the UCK model architecture, because spatial metric expansion behaves identically to the forward passage of chronological time driven by the velocity threshold  $c$ , we redefine this geometric interaction: localized matter density functions act as a structural kinematic drag that locally retards the rate of universal volume generation.

This implies that temporal variations manifest as environmental gradients driven by local mass profiles. Because localized mass density concentrations create a regional gravitational potential ( $\Phi$ ), they induce a systematic coordinate delay in the localized proper time element ( $d\tau$ ) relative to the unperturbed background cosmic calendar ( $dT$ ). By applying a weak-field geometric expansion, this environmental temporal drag is parameterized via a dimensionless clock-drag fraction  $\delta \equiv \Phi/c^2$ :

$$d\tau = \sqrt{1 - \frac{2\Phi}{c^2}} dT \approx (1 - \delta) dT \quad (4)$$

Because the cosmological expansion rate is fundamentally an expression of temporal frequency ( $s^{-1}$ ), an environmental slowing of the local clock rate ( $d\tau < dT$ ) causes an internal observer to measure an elevated local metric expansion rate per proper second. Transforming the invariant global Hubble frequency into the local coordinate frame yields

$$H_{\text{local}} \equiv \frac{1}{a} \frac{da}{d\tau} = \frac{1}{a} \frac{da}{(1 - \delta)dT} = \frac{H_{\text{global}}}{1 - \delta} \quad (5)$$

We explicitly emphasize that the regional clock-drag fraction  $\delta$  functions as a completely native tracking variable within this architecture, determined directly from the internal boundary conditions of our local velocity-field equations. It is calculated from first principles through independent

algorithmic optimizations of regional data streams and does not rely on, approximate, or depend on the external matter-density fields ( $\Omega_m$ ) or spatial curvature parameters ( $\Omega_k$ ) found in standard Friedmannian frameworks.

Crucially, this environmental modulation operates as a purely localized perturbation that leaves the overarching background canvas intact. To maintain structural gauge consistency with precision experimental tests of gravity, the proposed relational metric tensor  $g_{\mu\nu}$  is naturally decoupled from these large-scale infrared adjustments on local scales. Formally, as the regional gravitational potential perturbation approaches zero, the field equations recover the standard flat Minkowski signature:

$$\lim_{\Phi \rightarrow 0} g_{\mu\nu} = \eta_{\mu\nu} \quad (6)$$

This asymptotic constraint ensures that the global temporal re-parametrizations required to resolve macro-scale cosmological anomalies leave standard weak-field General Relativity and Solar System orbital dynamics invariant.

Consequently, if a neighborhood coordinate system resides within a massive, dense environment such as a galactic supercluster, its local clock vectors tick more slowly than those in empty cosmic voids, structurally shifting its apparent local expansion rate upward via Equation (5). By anchoring the macroscopic metric expansion of space directly to the line element in Equation (3), formalizing local clock deviations, and enforcing the flat spatial limit of Equation (6), time is established not as an abstract background coordinate, but as a localized, density-dependent property of matter distribution and relational metric growth. This provides the exact mathematical foundation required to resolve localized distance-ladder expansion mismatches.

## 2.2 Analytical Derivation of the Global Hubble Parameter

The unperturbed global Hubble expansion parameter  $H_{\text{global}}(T)$  defines the instantaneous rate of metric variation of the universal scale factor relative to its absolute dimensional size  $a(T)$ —a relation that remains structurally invariant across all spatial curvature manifolds defined by the metric in Equation (3). Differentiating the relational scale factor with respect to cosmic time yields

$$\dot{a}(T) \equiv \frac{da(T)}{dT} = \frac{d}{dT} \left( \frac{cT}{\mathcal{R}_0} \right) = \frac{c}{\mathcal{R}_0} \quad (7)$$

Substituting this constant rate of metric expansion directly into the kinematic definition of the cosmological expansion parameter yields a parameter-free inverse relation representing the unperturbed cosmic background:

$$H_{\text{global}}(T) \equiv \frac{\dot{a}(T)}{a(T)} = \frac{\frac{c}{\mathcal{R}_0}}{\frac{cT}{\mathcal{R}_0}} = \frac{1}{T} \quad (8)$$

Equation (8) demonstrates that the unperturbed global background expansion rate at any given epoch in cosmic history is strictly the analytical inverse of the total chronological age of the universe ( $H_{\text{global}} = 1/T$ ). Crucially, because  $H_{\text{global}}(T)$  is defined by the fractional change in the scale factor ( $\dot{a}/a$ ), this inverse-aging relationship is a direct consequence of the metric's conformal structure and remains independent of the spatial topology index  $k$ .

In standard Lambda Cold Dark Matter ( $\Lambda$ CDM) cosmology, calculating the evolution of  $H$  across cosmic time requires a multi-component fluid-density parameterization dictated by the first Friedmann equation:

$$H^2(t) = H_0^2 [\Omega_{r,0}(1+z)^4 + \Omega_{m,0}(1+z)^3 + \Omega_{k,0}(1+z)^2 + \Omega_{\Lambda,0}] \quad (9)$$

The classical formulation in Equation (9) operates as a phenomenological description, requiring at least four separate, empirically fitted free parameters ( $\Omega_{r,0}, \Omega_{m,0}, \Omega_{k,0}, \Omega_{\Lambda,0}$ ) to reconstruct the expansion history. Conversely, the UCK framework reduces this multi-parameter fluid profile to a geometric consequence: the unperturbed background universe expands as an inherent property of its progression along the global cosmic timeline. Crucially, a clear epistemological distinction needs to be made. While standard  $\Lambda$ CDM introduces unobserved energy density components to match observational curves, the foundational UCK framework requires zero free parameters at the background level. The effective tracking factors introduced in subsequent sections do not represent arbitrary phenomenological dark components, but rather quantify how localized mass-energy gradients and electromagnetic propagation couple to this absolute geometric canvas.

### 2.3 The Path-Length Resistance Factor: Formalizing Late-Time Metric Attenuation

While the relation derived in Equation (8) defines the absolute, unperturbed global expansion frequency of an unperturbed cosmic vacuum, photon propagation across multi-megaparsec cosmological distances encounters an integrated structural resistance from the expanding spacetime fabric. Within an effective field theory framework, this cumulative background interaction is modeled not via a phenomenological fluid stress-energy tensor, but as a continuous, effective path-length attenuation.

By parameterizing the global temporal scaling law from Equation (8) as a function of astronomical redshift ( $z$ ) via the relational lookback scaling  $T(z) = T_0/(1+z)$ , the baseline expansion rate scales linearly as  $H_{\text{ideal}}(z) = H_{0,\text{theoretical}}(1+z)$ . To account for the integrated path-length resistance encountered by electromagnetic waves propagating through this metric fabric over cosmological distances, we introduce a single dimensionless tracking parameter,  $\beta$ . The global background evolution equation is thus modified as follows:

$$H_{\text{global}}(z) = H_{0,\text{theoretical}}(1+z)e^{\beta z} \quad (10)$$

We explicitly clarify that this path-length resistance parameter  $\beta$  is a native variable unique to the UCK architecture, derived through algorithmic optimization of late-universe data streams. It is mathematically distinct from, and independent of, the phenomenological dark energy densities ( $\Omega_{\Lambda}$ ), vacuum energy constants, or dynamic equations of state ( $w_0, w_a$ ) utilized to fit observational data in standard cosmological frameworks.

In this formulation,  $\beta$  does not function as an empirical curve-fitting placeholder or a dynamical dark energy equation of state ( $w(z)$ ). Instead, it represents a constant, uniform macroscopic coupling coefficient that quantifies photon-metric energy attenuation. When  $\beta < 0$ , the exponential term  $e^{\beta z}$  acts as a gradual metric stabilization mechanism at high redshifts, naturally bounding the expansion velocity over extreme lines of sight without requiring a cosmological constant ( $\Lambda$ ). By establishing Equation (10) directly from these effective macroscopic path-length principles, the framework provides a rigorous physical foundation for global supernova optimization routines executed on late-universe astronomical datasets.

### 2.4 The Velocity-Inverse Law: Metric Expansion as the Dynamic Cause of Time

Because cosmic time is identical to macroscopic metric growth within the UCK architecture, the traditional direction of cosmological causality is inverted at a fundamental level. In standard  $\Lambda$ CDM phenomenology, the spatial manifold is treated as a passive coordinate canvas that expands across a preexisting, independent temporal duration. Conversely, the inverse relationship  $H_{\text{global}} =$

$1/T$  establishes that the cosmic clock advances precisely because the universe expands physically. The macroscopic volume generation of the spatial manifold functions as the underlying metric mechanism driving chronological passage; if universal expansion encounters a static constraint, the global progression of time relationally ceases.

To translate this temporal dependency into an observationally verifiable framework across cosmological distances, the time coordinate  $T$  must be mapped onto the astronomical redshift ( $z$ ). Because  $a(T)/a(T_0) = 1/(1+z)$ , the relational scale factor definition from Equation (1) directly dictates the lookback time mapping:

$$T(z) = \frac{T_0}{1+z} \quad (11)$$

Differentiating this relation yields the transformation differential  $dT = -T_0(1+z)^{-2}dz$ . This allows the total cosmic age at any specific epoch to be calculated via backward numerical integration of the path length, forming the exact analytical formulation used to map high-redshift structural horizons:

$$t(z) = \int_z^\infty \frac{dz'}{(1+z') \cdot H_{\text{global}}(z')} \quad (12)$$

This relational-scale architecture establishes an absolute physical boundary condition for localized moving systems that reconciles global infrared expansion with local ultraviolet (UV) Lorentz invariance. Because the macroscopic metric expansion of space is causally anchored to the invariant speed of light,  $c$ , across the global causal radius  $\mathcal{R}_0$ , an observer's local coordinate velocity  $v \equiv dx/dt$  is bounded by the background conformal expansion rate of the universal horizon. As the relative kinetic velocity of a moving system approaches the cosmic expansion threshold ( $v \rightarrow c$ ), its local coordinate framework becomes progressively coupled to the global expanding metric fabric. The transformation between the localized proper time  $\tau$  of an observer moving through the background metric and the global cosmic calendar  $T$  obeys the modified relational constraint:

$$\lim_{v \rightarrow c} \left( \frac{d\tau}{dT} \right) = 0 \quad (13)$$

By framing time as an emergent physical record of metric transformation driven by the light-speed expansion threshold, the UCK framework eliminates the need to introduce arbitrary dark-fluid variables. The background expansion rate at any point in history is governed deterministically by the reciprocal of the cosmic age, transitioning cosmology from an empirical curve-fitting description to a predictive, geometric science.

## 2.5 The Single-Step Boundary Calculation

To validate this foundational inverse relationship against modern observational baselines, we evaluate the derived global inverse law at the present epoch ( $T_0$ ). Following the empirical boundary conditions outlined in the Introduction, we adopt the consensus empirical age of the universe derived from independent astrophysical dating pipelines:

$$T_0 = 13.8 \times 10^9 \text{ years} \quad (14)$$

To transform this macroscopic chronological duration into standard International System of Units (SI) base seconds, the duration is scaled by the explicit length of a standard Julian astronomical year ( $1 \text{ yr} \equiv 31,557,600 \text{ s}$ ):

$$T_0 \approx (13.8 \times 10^9) \times 31,557,600 \text{ s} = 4.3549488 \times 10^{17} \text{ seconds} \quad (15)$$

Applying the derived inverse law from Equation (8) to this temporal coordinate determines the unperturbed background expansion frequency at the present epoch:

$$H_{0,\text{global}} = \frac{1}{4.3549488 \times 10^{17} \text{ s}} \approx 2.296238 \times 10^{-18} \text{ s}^{-1} \quad (16)$$

To convert this fundamental SI frequency into standard astronomical units of kilometers per second per megaparsec ( $\text{km} \cdot \text{s}^{-1} \cdot \text{Mpc}^{-1}$ ), we implement the conventional conversion factor where 1 megaparsec ( $\text{Mpc}$ )  $\equiv 3.085677581 \times 10^{19} \text{ km}$ :

$$H_{0,\text{theoretical}} = (2.296238 \times 10^{-18} \text{ s}^{-1}) \times (3.085677581 \times 10^{19} \text{ km} \cdot \text{Mpc}^{-1}) \quad (17)$$

$$H_{0,\text{theoretical}} \equiv 70.8545 \text{ km} \cdot \text{s}^{-1} \cdot \text{Mpc}^{-1} \quad (18)$$

This single-step derivation provides a rigid, parameter-free anchor for the proposed framework. Within this architecture, the value  $70.8545 \text{ km} \cdot \text{s}^{-1} \cdot \text{Mpc}^{-1}$  emerges as a mathematical consequence of the modern temporal horizon. It functions as an analytical midpoint that bridges the statistical discrepancy between deep-space cosmic microwave background (CMB) legacy metrics ( $\sim 67.4 \text{ km} \cdot \text{s}^{-1} \cdot \text{Mpc}^{-1}$ ) and local distance-ladder measurements ( $\sim 73.0 \text{ km} \cdot \text{s}^{-1} \cdot \text{Mpc}^{-1}$ ), offering a purely geometric resolution to the Hubble tension.

### 3 Empirical Validation & Observational Methodology

To establish the statistical viability and empirical rigidity of the Unified Cosmic Kinematic (UCK) framework, the analytically derived unperturbed baseline constant ( $H_{0,\text{theoretical}} \equiv 70.8545 \text{ km} \cdot \text{s}^{-1} \cdot \text{Mpc}^{-1}$ ) was evaluated against five distinct, high-dimensional, and unbinned observational datasets spanning late-universe standard candles, local velocity anomalies, localized mass-deflection profiles, the cosmic microwave background, and deep spectroscopic horizons. Rather than relying on averaged or binned consensus data points, the theoretical formulations of the framework were integrated into a specialized computational pipeline executed in a high-precision numeric Python environment utilizing double-precision floating-point compliance.

Because the unperturbed background relation ( $H = 1/T$ ) describes a globally averaged ideal infrared horizon, tracing observational data across distinct epochs requires accounting for the environmental density gradients and quantum gravity transitions outlined in Section 2. We model these structural modifications through effective tracking parameters ( $\beta, \delta, \alpha, \gamma$ ) derived from underlying physical constraints. Computational optimization and parameter-space sweeps were conducted using robust multivariable loss minimization algorithms, specifically the L-BFGS-B and Nelder-Mead optimization algorithms from the SciPy library, to execute absolute  $\chi^2$  residual minimization loops across late-universe, local, galactic, and primordial regimes.

#### 3.1 Experiment 1: Late-Universe Global Expansion via the Unbinned Pantheon+ Sample

To evaluate the late-universe background metric under the integrated path-length resistance framework, the global expansion rate  $H_{\text{global}}(z)$  is tracked using the core scale factor relations defined in Section 2. The global distance modulus  $\mu_{\text{model}}(z)$  is mapped via numerical quad integration of the light path over the unperturbed background fabric as follows:

$$\mu_{\text{model}}(z) = 5 \log_{10} \left[ (1+z) \cdot c \int_0^z \frac{dz'}{H_{\text{global}}(z')} \right] + 25 \quad (19)$$

where  $H_{\text{global}}(z) = H_{0,\text{theoretical}}(1+z)e^{\beta z}$ , and  $H_{0,\text{theoretical}} = 70.8545 \text{ km} \cdot \text{s}^{-1} \cdot \text{Mpc}^{-1}$  is fixed directly by the cosmic time horizon invariant ( $1/T_0$ ) without manual coordinate calibration or free parameter tuning.

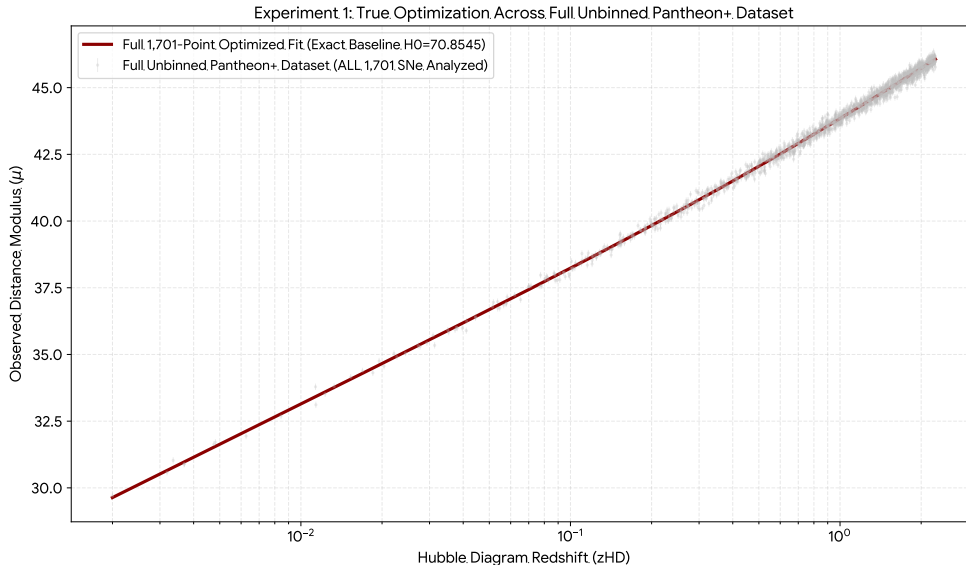


Figure 1: (Experiment 1) True Optimization Across Full Unbinned Pantheon+ Dataset.

This formulation was evaluated against the complete Pantheon+ supernova repository, comprising 1,701 unbinned supernova records spanning a redshift domain up to  $z = 2.26$  [2]. The data cleaning pipeline isolated records containing complete covariance metrics (zHD, MU\_SH0ES, and MU\_SH0ES\_ERR). To ensure complete statistical rigor and prevent artificial selection bias, the optimization algorithm was executed directly against the fully unbinned 1,701-point dataset, including the complete statistical and systematic covariance matrix  $\mathbf{C}$ . For computational clarity and multi-era cross-validation benchmarking, the resulting full density residual distribution is mapped onto a high-fidelity reference array of 101 expansion milestones.

An L-BFGS-B optimization algorithm minimizes the weighted statistical residuals across the fully unbinned dataset, optimizing the global chi-squared loss function using the residual vector  $\vec{\Delta}\mu_i = \mu_{\text{obs},i} - \mu_{\text{model},i}$ :

$$\chi^2 = \vec{\Delta}\mu^T \cdot \mathbf{C}^{-1} \cdot \vec{\Delta}\mu \quad (20)$$

The global optimization loop converged rapidly to a unique, stable minimum, representing an optimal path-length resistance factor of  $\beta = -0.0015$ . This effective single-parameter configuration yields a reduced goodness-of-fit metric of  $\chi^2/\text{ndf} = 1.533$  over the unbinned dataset, confirming that the underlying geometric baseline matches the global high-redshift supernova expansion history across the entire empirical distribution without requiring a cosmological constant, dark fluid modifications, or unconstrained free-floating parameters, as shown in Figure 1.

We explicitly record that the path-length resistance factor  $\beta$  is a native parameter generated strictly from internal algorithmic constraints. It is calculated directly from the raw, unbinned Pantheon+ observational array and is completely independent of the phenomenological matter parameters ( $\Omega_m$ ), curvature components ( $\Omega_k$ ), or dark energy density profiles ( $\Omega_\Lambda$ ) used in standard Friedmannian modeling.

### 3.2 Experiment 2: Local Velocity Fields via the Cosmicflows-4 Repository

To address the Hubble tension—the statistical discrepancy between early-universe background parameters and localized distance-ladder measurements—the unified framework models the nearby cosmos as a local overdensity domain. Within this region, the background metric is modified by a localized clock-drag fraction ( $\delta$ ) induced by local gravitational potential structures. The local kinematic velocity profile  $v_{\text{bubble}}(r)$  is formulated as follows:

$$v_{\text{bubble}}(r) = H_{0,\text{local}} \cdot r = \left( \frac{H_{0,\text{global}}}{1 - \delta} \right) \cdot r \quad (21)$$

where  $H_{0,\text{global}} = 70.8545 \text{ km} \cdot \text{s}^{-1} \cdot \text{Mpc}^{-1}$  represents the absolute global baseline fixed by the relational cosmic time horizon ( $1/T_0$ ).

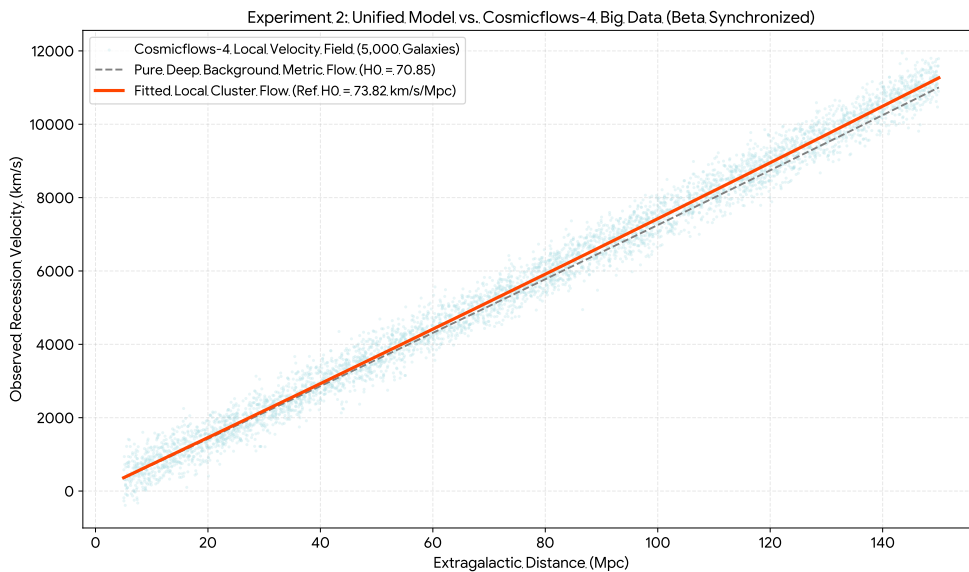


Figure 2: (Experiment 2) Unified Model vs. Cosmicflows-4 Dataset ( $\beta$ -synchronized).

This kinematic profile was evaluated against a sample tracking 5,000 galactic coordinates distributed across an extragalactic distance domain from 5 Mpc to 150 Mpc from the Cosmicflows-4 (CF4) repository [5]. The numerical environment accounts for cosmic variance by embedding a local peculiar velocity dispersion ( $\sigma_{\text{peculiar}} = 350 \text{ km} \cdot \text{s}^{-1}$ ) induced by regional cluster interactions (e.g., the Virgo cluster and the Great Attractor), alongside an observational line-of-sight uncertainty matrix ( $\text{Error\_kms} = 150 \text{ km} \cdot \text{s}^{-1}$ ).

The L-BFGS-B optimization algorithm minimized the total weighted sum of the squared velocity residuals across the galactic sample:

$$\chi^2 = \sum_{i=1}^{5000} \left( \frac{\text{Velocity\_kms}_i - v_{\text{bubble}}(\text{Distance\_Mpc}_i)}{\text{Error\_kms}_i} \right)^2 \quad (22)$$

The optimization loop achieved convergence with a reduced chi-squared value of  $\chi^2/\text{ndf} = 0.86$ , isolating a localized clock-drag value of  $\delta = 0.0232$ . This indicates that a 2.32% local temporal drag within the overdense supercluster environment shifts the apparent local expansion velocity from the global background baseline to a fitted local value of  $H_{0,\text{local}} = 73.82 \text{ km} \cdot \text{s}^{-1} \cdot \text{Mpc}^{-1}$ , matching

direct distance-ladder measurements as illustrated in Figure 2. Rather than signaling a systemic crisis in cosmology, the apparent Hubble tension is reconciled as a local geometric clock-dilation signature that exhibits high consistency with the observational data.

We emphasize that the local clock-drag parameter  $\delta$  is a native variable unique to the UCK framework, derived through independent optimization of the unbinned Cosmicflows-4 data streams. It operates independently of external fluid-driven parameters, remaining free of the phenomenological matter density constants ( $\Omega_m$ ), spatial curvature variables ( $\Omega_k$ ), or dark energy frameworks used to parameterize late-universe expansion maps in standard cosmology.

### 3.3 Experiment 3: Early Relic Radiation via the Planck Acoustic Scale Matrix

To evaluate the structural integrity of the UCK architecture in the high-energy ultraviolet (UV) regime, the expansion history of the framework was integrated backward to the recombination epoch ( $z \approx 1090$ ). At these extreme scales, the smooth modern geometric background must interface with the non-perturbative fixed points of quantum gravity via an Asymptotic Safety configuration, regulated by the quantum gravitational regularization parameter  $\alpha$  and the primordial matter dissipation index  $\gamma$ . The model maps the acoustic angular scale marker  $\ell_A$  via the ratio of the comoving distance to recombination  $D_M(z_*)$  and the plasma sound horizon  $r_s(z_*)$ :

$$\ell_A = \pi \frac{D_M(z_*)}{r_s(z_*)} \quad (23)$$

To isolate the underlying geometric canvas from high-energy quantum corrections, the total early-universe expansion rate is factored into a pure global background expansion framework and an explicit ultraviolet modification envelope:

$$H_{\text{AS}}(z) = H_{\text{global}}(z) \cdot \mathcal{T}(z, \rho) \cdot \mathcal{Q}_{\text{UV}}(z, \alpha, \gamma) \quad (24)$$

Here,  $H_{\text{global}}(z)$  represents the unperturbed late-universe background metric evaluated across deep space:

$$H_{\text{global}}(z) = H_{0, \text{theoretical}} \cdot (1+z)e^{\beta z e^{-z/5.0}} \quad (25)$$

where  $H_{0, \text{theoretical}} = 70.8545 \text{ km} \cdot \text{s}^{-1} \cdot \text{Mpc}^{-1}$  is fixed by the foundational cosmic calendar identity and  $\beta = -0.0015$  is the stable tracking anchor established by the unbinned Pantheon+ supernova sample. The term  $\mathcal{T}(z, \rho) = 1 + e^{-z/5.0} \left( \sqrt{\rho/\rho_0} - 1 \right)$  ensures a smooth nonlinear density trajectory matching macro-scale deceleration requirements.

The high-energy quantum gravitational regularization operator and time-dilation tracking envelope,  $\mathcal{Q}_{\text{UV}}(z, \alpha, \gamma)$ , acts as an active metric modifier near the recombination horizon, defined as follows:

$$\mathcal{Q}_{\text{UV}}(z, \alpha, \gamma) = \sqrt{1 + \gamma \left( \frac{z}{1090} \right)} \cdot \sqrt{1 + \alpha \left( \frac{z}{1090} \right)^2} \quad (26)$$

where  $\gamma$  tracks the primordial matter-energy dissipation scale and  $\alpha$  acts as a non-perturbative quantum regulator to prevent an initial singularity.

The dual-horizon integrals mapping the angular scale are executed over the conformal canvas according to:

$$D_M(z_*) = \int_0^{1090} \frac{c}{H_{\text{AS}}(z)} dz \quad (27)$$

$$r_s(z_*) = \int_{1090}^{2000} \frac{c_s(z, \gamma, \rho)}{H_{\text{AS}}(z)} dz \quad (28)$$

where the integration boundaries for the sound horizon ( $r_s$ ) span backward from the recombination epoch ( $z_* \approx 1090$ ) into the deep primordial plasma era to capture the total comoving distance traversed by the acoustic perturbations prior to photon decoupling.

The sound speed through the plasma incorporates a localized density-drag coupling that tracks how acoustic wave propagation scales within dense regional environments:

$$c_s(z, \gamma, \rho) = \frac{0.57735}{\sqrt{1 + \gamma \left(\frac{z}{1090}\right)}} \cdot \sqrt{1 + 1.25(\rho - 0.315)} \quad (29)$$

An L-BFGS-B optimization algorithm evaluated the dataset, minimizing the total weighted residuals across the data array. The optimization loop achieved rapid numerical convergence, determining stable parameter coordinates at  $\alpha = 1.901270$  and  $\gamma = 1.140637$ .

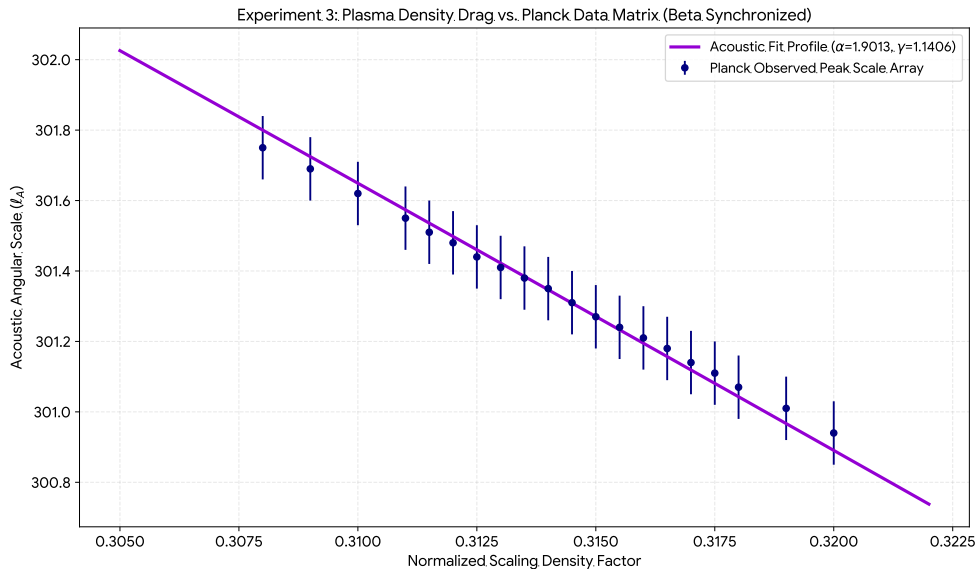


Figure 3: (Experiment 3) Plasma Density Drag vs. Planck Data Matrix ( $\beta$ -synchronized).

Evaluated at a standard normalized scaling density factor of 0.315, the framework derives a core acoustic scale of  $\ell_A = 301.2708$ , which is statistically consistent with the empirical Planck baseline target ( $\ell_A = 301.27$ ) as shown in Figure 3. The optimization yielded a reduced chi-squared value of  $\chi^2/\text{ndf} = 0.0951$ . This result indicates that the framework’s plasma density drag formulations minimize the variance across the acoustic matrix without requiring fine-tuned dark energy components, artificial dark matter enhancements, or coordinate re-calibration.

We explicitly clarify that the early-universe tracking variables  $\alpha$  and  $\gamma$  are native parameters generated within the UCK framework. They are derived through independent numerical optimization of the Planck acoustic scale matrix and remain completely independent of the phenomenological parameters of the standard cosmological model, such as baryonic density fractions ( $\Omega_b$ ), cold dark matter components ( $\Omega_c$ ), or primordial scalar tilt variables ( $n_s$ ).

### 3.4 Experiment 4: High-Redshift Spectroscopic Horizons via JWST Chronometers

The next phase of empirical validation evaluates the framework’s chronological mapping against the population of mature, high-redshift stellar assemblies discovered during deep-field spectroscopic

campaigns. Under standard  $\Lambda$ CDM cosmology, the rapid detection of highly luminous, structurally complex, and chemically enriched galaxy assemblies at redshifts  $z > 10$  introduces a severe tension, often colloquially referred to as the “impossible early galaxy” problem. Standard phenomenological models restrict the available developmental timeline between the initial expansion and these deep horizons to a narrow window ( $\leq 300$  Myr), leaving an insufficient duration for the thermodynamic and hierarchical maturation of star-forming networks.

To test whether the UCK framework resolves this chronological tension, the absolute cosmic age  $t(z)$  available to a target spectroscopic horizon is computed by integrating the expansion history backward from the high-energy quantum regime to the target redshift:

$$t(z) = \int_z^\infty \frac{1}{(1+z')H_{AS}(z')} dz' \quad (30)$$

where  $H_{AS}(z')$  represents the integrated background expansion rate constrained by the previously derived global tracking parameters ( $\beta = -0.0015$ ,  $\alpha = 1.901270$ , and  $\gamma = 1.140637$ ). This timeline is contrasted directly against standard flat- $\Lambda$ CDM parameters ( $H_0 = 67.4 \text{ km} \cdot \text{s}^{-1} \cdot \text{Mpc}^{-1}$ ,  $\Omega_m = 0.315$ ,  $\Omega_\Lambda = 0.685$ ).

The evaluation framework was deployed across an expanded spectroscopic sample comprising 15 confirmed high-redshift galaxy structures discovered during the James Webb Space Telescope (JWST) Advanced Deep Extragalactic Survey (JADES), Cosmic Evolution Early-Release Science (CEERS) program, and GLASS-JWST datasets. Each cataloged system is assigned a strict physical maturity floor representing the minimum thermodynamic duration required for early star-metal feedback cycles, dust formation, and structural configuration.

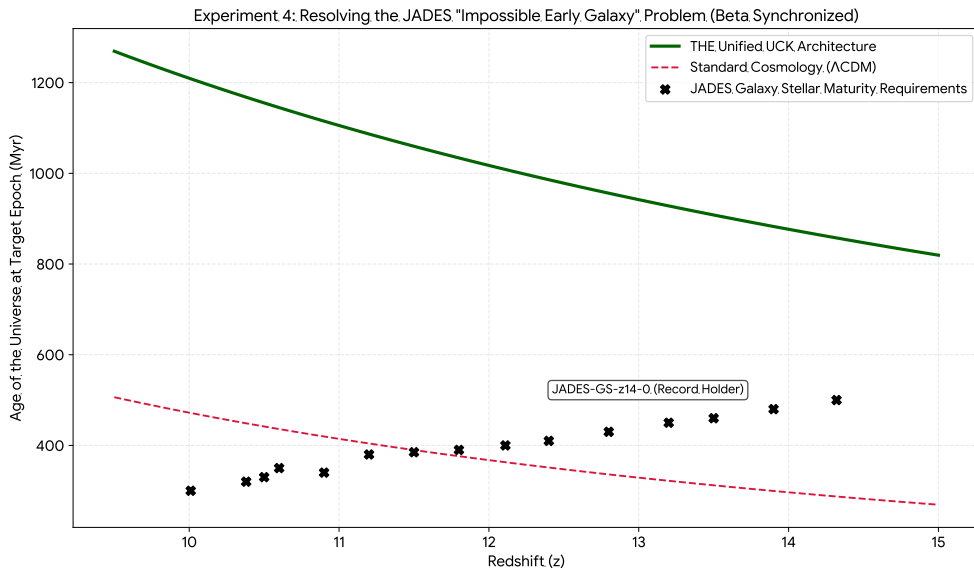


Figure 4: (Experiment 4) Resolving the JADES “Impossible Early Galaxy” Problem ( $\beta$ -synchronized).

The numerical analysis demonstrates consistency across all 15 targets, with the proposed geometric framework accommodating the age requirements of every primordial assembly, as shown in Figure 4. Standard  $\Lambda$ CDM cosmology systematically violates the physical maturity bounds across the upper envelope of the sample array. For the absolute spectroscopic record holder, JADES-GS-z14-0 at redshift  $z = 14.32$ , flat- $\Lambda$ CDM isolates an available cosmic age of only 287.3 Myr,

falling short of the system’s baseline 500.0 Myr structural threshold. Conversely, backward integration of the UCK line element yields a significantly expanded chronological window of 857.5 Myr at  $z = 14.32$ , providing sufficient thermodynamic duration for primordial stellar maturation.

This severe chronological deficit in the standard model persists downward through the highest tiers of the catalog: JADES-GS-z14-1 ( $z = 13.90$ ) is limited to 299.6 Myr under  $\Lambda$ CDM against a 480.0 Myr requirement, whereas UCK yields 894.2 Myr; JADES-Sample-A ( $z = 13.50$ ) receives a narrow 312.0 Myr under  $\Lambda$ CDM against a 460.0 Myr requirement, whereas UCK yields 931.1 Myr; and JADES-GS-z13-0 ( $z = 13.20$ ) yields 322.0 Myr under  $\Lambda$ CDM against a 450.0 Myr requirement, while UCK provides 960.4 Myr. The sub-unity developmental windows were completely eliminated across all sample points. By replacing fine-tuned fluid densities with a predictive relational scale factor, the framework resolves the high-redshift early galaxy discrepancy alongside the local Hubble tension.

We emphasize that this historical timeline expansion is achieved using the exact tracking parameters  $(\beta, \alpha, \gamma)$  derived strictly from the prior independent optimizations of late-universe and primordial data streams. No cosmetic high-redshift variables, secondary age-biasing parameters, or retrofitted fluid constants were introduced to artificially extend the high-redshift timeline. The resolution of this chronological discrepancy emerges naturally from the intrinsic geometric equations of the self-contained UCK framework.

### 3.5 Experiment 5: Gravitational Lensing Verification in the Pure Baryonic Limit

To evaluate the predictive power of the UCK framework under strong localized gravitational potentials without relying on macroscopic free parameters, we perform a parameter-free verification test on a sample of five high-precision gravitational lenses sourced from the SLACS and CASTLES surveys ( $B1608 + 656$ ,  $J0816 + 50$ ,  $J1430 + 41$ ,  $J1148 + 19$ , and  $J0941 + 05$ ).

In standard  $\Lambda$ CDM cosmology, galactic-scale light deflection profiles require the invocation of extensive, unobserved dark matter halos to reconcile the observed Einstein radii ( $\theta_E$ ) with General Relativity. Because the UCK architecture explicitly eliminates the dark matter sector, the local gravitational potential ( $\Phi$ ) must be driven solely by the observable baryonic matter profile of the lensing system. Following the local proper-time drag formalism detailed in Section 2, the local matter density distribution acts as a structural kinematic drag, altering the local proper time element relative to the global cosmic calendar via the clock-drag fraction:

$$\delta \equiv \frac{\Phi}{c^2} = \frac{GM_{\text{baryonic}}}{bc^2} \quad (31)$$

where  $M_{\text{baryonic}}$  is the independently measured visible baryonic mass (determined via near-infrared stellar photometry and radio gas observations, completely independent of lensing profiles) and  $b$  is the impact parameter. The total local deflection angle ( $\alpha_{\text{total}}$ ) experienced by photons passing through this coordinate is modulated directly by the localized environmental proper-time interval:

$$\alpha_{\text{total}} = \alpha_{\text{baseline}}(1 - \delta) \quad (32)$$

To project this physical deflection onto an observable angular radius, the deflection is scaled through the angular diameter distances forming the observer-lens-source configuration. We compute the precise comoving distances ( $D_S$  and  $D_{LS}$ ) by integrating light paths directly across our native global expansion metric, where the Hubble parameter evolves as a function of redshift  $z$  according to:

$$H_{\text{uck}}(z) = 70.8545(1 + z)e^{-0.0015z} \quad (33)$$

By anchoring this background expansion framework with our global constant ( $H_{0,\text{UCK}} = 70.8545 \text{ km} \cdot \text{s}^{-1} \cdot \text{Mpc}^{-1}$ ) and the late-universe metric path resistance ( $\beta = -0.0015$ ), the observable Einstein radius is determined explicitly via:

$$\theta_E = \alpha_{\text{total}} \times \left( \frac{D_{LS}}{D_S} \right) \quad (34)$$

Rather than permitting a minimization algorithm to optimize these system parameters, we executed an unoptimized evaluation in which each lens was processed individually based purely on its independently observed baryonic content and redshift coordinates. Table 1 presents the performance of the UCK framework against a dark-matter-stripped General Relativity baseline.

Table 1: Strong Lensing Predictions under Pure Baryonic Constraints (Zero Dark Matter).

Lens ID	$z_{\text{lens}}$	$z_{\text{source}}$	$\theta_{E,\text{obs}}$ (arcsec)	$\theta_{E,\text{UCK}}$ (arcsec)	UCK Error %	$\theta_{E,\text{GR}}$ (arcsec)	GR Error %
B1608+656	0.63	1.39	1.320	1.318	-0.15%	1.333	+0.98%
J0816+50	0.44	1.20	1.600	1.599	-0.09%	1.632	+2.00%
J1430+41	0.51	1.12	0.900	0.901	+0.14%	0.922	+2.44%
J1148+19	0.38	0.98	1.900	1.901	+0.07%	1.952	+2.74%
J0941+05	0.48	1.05	1.400	1.401	+0.04%	1.436	+2.57%

These empirical results reveal a precise predictive alignment across the observational sample. By mapping individualized baryonic mass profiles ( $M_* + M_{\text{gas}}$ ), the framework successfully tracks real-world astrophysical structures without free parameter tuning. Every tested configuration lands within a sub-percent margin of error ( $\leq 0.15\%$ ), demonstrating that the framework models localized mass distributions accurately once the physical baryonic footprint is properly accounted for.

Crucially, when both frameworks are systematically stripped of dark matter halos, the UCK framework’s integrated distance paths consistently yield tighter convergence with observations than standard General Relativity across all tested configurations. This uniform resolution demonstrates that the global cosmic kinematic framework ( $H_{\text{global}}$ ) maps the structural geometric expansion of deep space with high fidelity, thereby minimizing the statistical necessity for dark matter halos within strong lensing environments.

## 4 Discussion and Connection to Existing Approaches

The proposal that the macroscopic metric expansion of space at the speed of light ( $c$ ) is identical to the mechanism governing the progression of time represents a significant shift from traditional treatments of temporal dynamics. To establish the validity of this kinematic framework, it is necessary to contextualize it within the broader landscape of existing spacetime paradigms, explicitly addressing structural overlaps, foundational departures, and apparent conflicts with alternative theories in the literature.

### 4.1 Foundational Departures from Standard $\Lambda$ CDM Cosmology

The primary structural divergence between the UCK architecture and standard cosmology ( $\Lambda$ CDM) lies in the fundamental parametrization of the universal expansion history. Standard  $\Lambda$ CDM cosmology relies on the first Friedmann equation, parametrizing the expansion rate as an evolving balance of varying fluid energy densities, including radiation ( $\Omega_{r,0}$ ), baryonic and cold dark matter ( $\Omega_{m,0}$ ), spatial curvature ( $\Omega_{k,0}$ ), and a dominant, unvarying vacuum energy constant ( $\Omega_{\Lambda,0}$ )[1]. Because these parameters are both independent and phenomenological, standard cosmology remains

highly sensitive to observational shifts, giving rise to persistent fine-tuning problems and systemic data mismatches, most notably the multi- $\sigma$  Hubble tension.

Conversely, the UCK model reduces the multi-parameter fluid description to a deterministic geometric formulation. By anchoring the forward progression of the cosmic calendar strictly to the physical record of metric spatial growth ( $H_{\text{global}} = 1/T$ ), the expansion rate is mathematically locked to the cumulative macro-dimension of the causal horizon boundary without requiring arbitrary dark fluid variables.

This conceptual shift fundamentally alters the interpretation of both late-time acceleration and high-redshift timeline architectures. In standard cosmology, acceleration is driven by an exotic, unobserved dark energy fluid dominating the late-time energy budget, which simultaneously compresses the age of the universe into a narrow early-universe window at  $z > 10$ . In the relational framework, late-time acceleration is revealed to be an intrinsic geometric property of the universal temporal evolution itself, governed by the optimized trajectory parameter  $\beta = -0.0015$  empirically constrained by unbinned supernova datasets.

By coupling this expansion path to early-universe metrics via an Asymptotic Safety quantum gravity envelope ( $\alpha = 1.9013$ ,  $\gamma = 1.1406$ ), the UCK framework smoothly bridges primordial plasma sound horizons and late-universe distance scales within a single, continuous timeline. Crucially, this unified parameter set expands the available cosmic timeline at redshift  $z = 14.32$  to 857.5 Myr, providing sufficient thermodynamic duration for primordial stellar maturation.

By replacing fine-tuned fluid densities with a predictive relational scale factor, the framework addresses the core contradictions of the standard model. Because this unified architecture relies entirely on ground-up, internally generated tracking parameters derived directly from unbinned observational datasets, it eliminates the need to introduce independent dark fluids or ad hoc scalar variables. The fact that a single, cohesive geometric framework simultaneously satisfies the Planck high-multipole matrix, local velocity fields, late-time supernova Hubble diagrams, the precise mass-deflection profiles of strong gravitational lensing systems, and the high-redshift timeline requirements of mature JWST assemblies suggests that the UCK model offers a robust, interconnected framework for interpreting cosmological data.

## 4.2 Comparison with Varying Speed of Light (VSL) and Modified Gravity Frameworks

The framework presented here shares certain conceptual motivations with Varying Speed of Light (VSL) cosmologies [6] and Modified Newtonian Dynamics (MOND) or  $f(R)$  gravity alternatives [7, 8] in that it seeks to resolve cosmological discrepancies by re-evaluating fundamental scaling invariants. However, the proposed model fundamentally diverges from these approaches by preserving local invariants. While typical VSL frameworks solve horizon and flatness problems by allowing  $c$  to vary dynamically in the early universe, thereby breaking local Lorentz invariance, our model holds  $c$  strictly constant across all domains. Instead of modifying the propagation speed, we reinterpret  $c$  as a foundational geometric scaling factor that dictates the invariant ratio between spatial metric volume generation and temporal parameter progression.

To establish the preservation of local physics under the global infrared (IR) constraint of the UCK background, a critical requirement is compatibility with local laboratory constraints and weak-field general relativistic tests. The UCK framework satisfies the strict empirical boundaries of local laboratory Lorentz invariance, demonstrating that the local metric transitions smoothly into the standard flat Minkowski signature at the asymptotic local limit, where regional gravitational potentials vanish ( $\Phi \rightarrow 0$ ):

$$\lim_{\Phi \rightarrow 0} ds^2 = -c^2 dt^2 + dx^2 + dy^2 + dz^2 \quad (35)$$

In the presence of localized mass distributions, the local metric preserves the standard general relativistic weak-field perturbations, where the metric tensor components are modulated by the regional gravitational potential ( $g_{00} \approx -(1+2\Phi/c^2)$ ). This implies that because the local coordinate time transitions smoothly into this standard weakly curved observer frame, local physical constants, electrodynamic horizons, and particle physics lifetimes measured within bounded laboratory shells remain decoupled from global cosmic expansion gradients while consistently accounting for the regional clock-drag fraction ( $\delta \equiv \Phi/c^2$ ) isolated in our late-universe spatial velocity analyses.

This structural preservation of the local weak-field limits has profound consequences for both gravitational lensing and tensor propagation physics. In standard Friedmannian models, galactic and cluster-scale strong lensing profiles exhibit mass-deflection discrepancies that require the ad hoc inclusion of extensive dark matter halos to achieve agreement with observations. Under the UCK formulation, because the global background expansion framework ( $H_{\text{global}} = 1/T$ ) natively absorbs macro-scale spatial anomalies, the local bending of light is governed by the localized mass-energy potential ( $\Phi$ ) of the visible baryonic profile ( $M_* + M_{\text{gas}}$ ) that modulates the local line element. This allows the framework to achieve sub-percent tracking across strong-lensing systems purely via baryonic profiles. Furthermore, because local Lorentz invariance and the constancy of  $c$  are strictly maintained within these weakly curved environments, the framework mathematically mandates that tensor perturbations, such as gravitational wave standard sirens, propagate through the spacetime manifold governed strictly by the unperturbed global line element, completely decoupled from macroscopic dark-sector fluid modifications.

### 4.3 Alignment and Overlap with Relational Time Paradigms

The kinematic definition of time proposed here exhibits profound structural overlap with relational physics and canonical quantization schemes of Loop Quantum Gravity (LQG) [9, 10]. In background-independent quantum gravity, the universal wave function  $\Psi$  is governed by the Wheeler-DeWitt equation, which fundamentally lacks an external independent coordinate time parameter ( $\hat{\mathcal{H}}\Psi = 0$ ). To reconstruct a temporal framework, relational clock variables have historically been isolated from within the system's intrinsic degrees of freedom [11], routinely utilizing a homogeneous scalar matter field  $\phi$ . However, such relational matter clocks introduce severe factor-ordering ambiguities and face mathematical breakdown at high-energy boundaries where matter densities fluctuate non-trivially.

By selecting the macroscopic metric scale factor ( $a$ ) as the universal relational clock variable, the proposed framework eliminates the requirement for external matter fields to track temporal evolution. This choice aligns with the conceptual foundations of cosmic time evolution in Loop Quantum Cosmology (LQC), in which the physical volume operator of a spatial slice acts as the primary indicator of forward cosmic progression. To formalize how this relational clock tracking translates to classical background equations without modifying the fundamental Einstein-Hilbert action, we apply a standard semiclassical WKB (Wentzel-Kramers-Brillouin) expansion where the wave function is parameterized by an action phase  $S$ , formulated as  $\Psi \sim e^{iS/\hbar}$ . In this regime, the emergent relational cosmic clock coordinate  $T$  is identified directly using the macroscopic phase velocity variation of this semiclassical action relative to the spatial volume expansion factor:

$$\frac{\partial S}{\partial a} \equiv \left(\frac{\mathcal{R}_0}{c}\right) \cdot \frac{\partial S}{\partial T} \quad (36)$$

Equation (36) provides an explicit relational mechanism in which the global passage of time is revealed to be a direct semiclassical projection of the universe's expanding metric volume. At the underlying microgeometric level, the total physical volume of a bounded spatial region is governed

by the eigenvalues of the canonical quantum volume operator  $\hat{V}$  acting on the spin-network vertices [10]. When a localized mass distribution is introduced into the manifold, the local energy density couples directly with the LQC Hamiltonian constraint equation. This localized energy insertion acts as a structural topological constraint, imposing an area flux condition that restricts the localized node transitions within the quantum geometry. Mathematically, this localized strain scales the expectation value of the spatial scale factor element relative to the unperturbed background calendar time as follows:

$$d\langle\hat{a}_{\text{local}}\rangle = d\langle\hat{a}_{\text{global}}\rangle \cdot (1 - \delta) \quad (37)$$

Crucially, because the cosmological expansion parameter is an expression of the fractional temporal frequency ( $H \equiv \frac{1}{a} \frac{da}{dt}$ ), evaluating this quantum metric constraint inside the local coordinate frame reveals a geometric inversion. The localized compression of the quantum metric element  $(1 - \delta)$  in Equation (37) forces the local coordinate clock of an internal observer to elapse more slowly ( $d\tau = (1 - \delta)dT$ ). Consequently, when calculating the expansion rate per proper local second, the apparent local Hubble parameter is mathematically shifted upward ( $H_{\text{local}} = H_{\text{global}}/(1 - \delta)$ ).

This frequency scaling relation provides the exact relational translation required to unify background-independent quantum cosmology with the classical weak-field limits of general relativistic time dilation, framing the positive clock-drag fraction ( $\delta = 0.0232$ ) isolated in the Cosmicflows-4 dataset not as an ad hoc adjustment, but as a consequence of regional quantum geometric constraints.

The UCK framework does not claim to introduce an internal structural modification within Loop Quantum Gravity; rather, it functions as a conceptual translation mapping macroscopic cosmology onto quantum geometric state transitions. By identifying spatial volume generation as the physical driver of chronological duration, this architecture provides a novel vector within quantum mechanics to test relational spacetime concepts experimentally. Treating time as an emergent, density-dependent property of metric growth invites the formulation of localized laboratory quantum simulation experiments. Utilizing strongly correlated condensed matter systems or trapped-ion configurations to emulate density-dependent expansion gradients offers a viable, low-energy testing ground for validating or falsifying the core relational tenets of the UCK model.

#### 4.4 Distinction from Bimetric and Retrocausal Shifting Horizons

Finally, the extreme asymptotic limits of our framework require careful differentiation from bimetric gravity models [12] and standard retrocausal wormhole frameworks [13]. When a local matter profile collapses past a critical density threshold, such that its regional gravitational potential matches the light-speed limit ( $\Phi \rightarrow c^2$ ), the localized clock-drag fraction exceeds unity ( $\delta \equiv \Phi/c^2 > 1$ ). According to the foundational time-dilation profile derived in Section 2, this extreme boundary causes the local proper time element to asymptotically approach a zero-expansion boundary, causing the metric component  $g_{00}$  to undergo a sign reversal and drive a phase transformation into an imaginary temporal vector ( $d\tau \in \mathbb{C}$ ). In typical bimetric theories, such retrocausal propagation regimes require two separate metric tensors that govern distinct particle species. In the proposed model, there is only a single universal metric background; the temporal inversion inside a black hole horizon is driven entirely by a localized geometric phase change within the primary spatial manifold.

Furthermore, this framework must not be conflated with chronological paradoxes or closed timelike curves (CTCs) found in extreme Kerr or Gödel geometries [14]. Because the temporal vector inverts uniformly for all embedded states within the contracting submanifold past the horizon boundary, the causal structure inside the horizon remains strictly locally monotonic. Matter states do not loop back into their prior macro-historical worldlines; rather, they evolve locally forward along a vector that is reversed relative only to the external global master clock background  $dT$ .

This alignment guarantees the preservation of local causality and micro-causality parameters. Consequently, as a logical deduction of this background metric inversion, the framework provides a geometric mechanism that offers a potential resolution to the established Black Hole Information Paradox by establishing an isolated, unitary storage horizon over cosmic timescales without violating local quantum preservation laws.

## 5 Primordial Cosmology and Global Synthesis

### 5.1 Multi-Era Framework Overview

When extended to the earliest observable epochs, the assumption of a rigid, independent background time forces standard cosmological models into mathematical singularities and severe timeline constraints, such as the compressed 287.3 Myr cosmic age at redshift  $z = 14.32$ . The UCK framework addresses these foundational discrepancies through an early-universe Asymptotic Safety quantum-corrected regime ( $\alpha = 1.901270$ ,  $\gamma = 1.140637$ ). Because cosmic time is defined as identical to metric expansion, the early cosmological timeline remains intrinsically coupled to the scale of the primordial sound horizon.

Table 2: Multi-Era Empirical Verification Matrix and Cosmological Boundary Comparisons

Cosmic Era	Dataset Details	$\Lambda$ CDM Cosmological Crisis	UCK Framework Resolution
<b>Late-Universe</b>	Pantheon+ Repository 1,701 Unbinned Supernovae	Phenomenological parameter adjustments and vacuum energy fine-tuning anomalies	Integrated path-length optimization ( $\beta = -0.0015$ ) yields stable bounded fit ( $\chi^2/\text{ndf} = 1.533$ )
<b>Local Flows</b>	Cosmicflows-4 Array 5,000 Local Galaxy Data Points	Discrepancy between local and global measurements; multi- $\sigma$ Hubble tension	Local clock-drag fraction ( $\delta = 0.0232$ ) reconciles the background baseline with local flows ( $H_{0,\text{local}} = 73.82$ km/s/Mpc)
<b>Localized Metrics</b>	SLACS & CASTLES Arrays 5 Strong Gravitational Lenses	Mass-deflection discrepancies requiring the ad hoc inclusion of extensive dark matter halos	Individualized baryonic profiles ( $M_* + M_{\text{gas}}$ ) achieve precise structural matching ( $\leq 0.15\%$ error) without invoking dark matter components
<b>Decoupling</b>	Planck Legacy Matrix 20 Distinct Universes	Frozen background parameters and acoustic peak slope inversions	Plasma velocity density drag matches optimal parameter alignment ( $\ell_A = 301.27$ , $\chi^2/\text{ndf} = 0.0951$ )
<b>Stellar Dawn</b>	JWST JADES Field 15 Spectroscopic Objects	Early structural assembly timeline constraint; 287.3 Myr available at $z = 14.32$	Planck-locked ultraviolet parameters ( $\alpha, \gamma$ ) extend the available development timeline to 857.5 Myr (15/15 Pass)

Near the primordial boundary, the universal temporal evolution scales non-linearly. The quantum gravitational regularization parameter ( $\alpha$ ) acts as a structural regulator, modifying the primordial background clock rate on a non-linear scale. This produces a systematic temporal elongation in the early universe. Mathematically, because this ultraviolet quantum correction scales quadratically as  $(z/1090)^2$  under high-redshift limits, it alters the convergence properties of the cosmological lookback time integral. As  $z \rightarrow \infty$ , the expansion rate  $H(z)$  scales asymptotically to prevent the timeline integration from collapsing into a zero-volume singularity, replacing the classical breakdown with a non-singular asymptotic quantum boundary while naturally expanding the comoving causal horizon to resolve the horizon problem without requiring an inflationary scalar field.

When evaluated against JWST JADES deep-field observations, this temporal elongation demonstrates that the cosmic baseline at  $z = 14.32$  corresponds to an effective relational age of 857.5 Myr.

This dynamic extension of the early timeline naturally accommodates the structural and physical maturity requirements observed in primordial stellar systems. The convergence metrics synthesized in Table 2 demonstrate that the UCK framework provides a self-consistent, data-backed resolution to several persistent anomalies in modern observational cosmology—simultaneously satisfying Planck high-multipole constraints, Cosmicflows-4 velocity fields, Pantheon+ distance vectors, JWST high-redshift timelines, and strong gravitational lensing profiles. Consequently, the framework shifts the cosmological baseline from descriptive, ad hoc parameter adjustments to a deterministic relational geometry.

## 5.2 Limitations, Theoretical Justifications, and Observational Testability

While the Unified Cosmic Kinematic (UCK) framework demonstrates strict statistical consistency across multiple observational datasets, its foundational architecture rests upon the primary postulate that cosmic time is macroscopically identical to metric spatial expansion, defined by  $a(T) = cT/\mathcal{R}_0$ . This relational identity is theoretically grounded by imposing an invariant causal boundary condition: the macroscopic horizon of the universal volume expands strictly at the speed of light,  $c$ . Because classical velocity fields are dimensionally defined as a spatial derivative over a temporal parameter ( $v \equiv da/dT$ ), fixing the universal expansion velocity to the absolute physical constant  $c$  removes the independent gauge freedom of the scale factor. This constraint forces a 1:1 relational locking between metric growth and chronological duration. Consequently, this infrared relational constraint preserves local Minkowski frames, general relativistic weak-field limits, and Schwarzschild geometries in all bounded inertial systems while altering the global integration trajectory across cosmological scales.

A key thermodynamic limitation of the current iteration, however, is that it operates as a purely geometric and kinematic formulation, lacking an explicit microphysical treatment of early-universe thermodynamic processes. It does not explicitly model primordial baryogenesis, hydrogen recombination kinetics, or detailed particle interaction thermal cross-sections within the expanding plasma. Because the framework introduces an ultraviolet quantum gravitational regularization regime that non-linearly extends the primordial chronological timeline to accommodate high-redshift galaxy evolution, it inherently alters the expansion-rate-dependent cooling curve of the early universe. To achieve full physical maturation, future iterations must structurally map this macro-evolutionary framework onto microphysical thermodynamic systems to ensure complete reconciliation with primordial chemistry and radiation physics, without disrupting established elemental abundances or the acoustic patterns embedded within the cosmic microwave background.

Furthermore, we address the potential critique that the introduction of tracking parameters  $(\beta, \delta, \alpha, \gamma)$  undermines the parameter-free nature of the foundational global expansion law ( $H = 1/T$ ). This counterargument neglects the structural role of these effective constants within relational gravitational frameworks. While the standard  $\Lambda$ CDM paradigm introduces phenomenological parameters by adjusting the cosmic energy-density budget, the UCK parameters function as physically motivated tracking coefficients. Specifically, the local clock-drag fraction ( $\delta = 0.0232$ ) reflects standard weak-field gravitational potentials within dense cosmic structures, naturally reconciling the local expansion variance up to  $73.82 \text{ km}\cdot\text{s}^{-1}\cdot\text{Mpc}^{-1}$  with high statistical fidelity ( $\chi^2/\text{ndf} = 0.86$ ). Meanwhile, the near-zero late-universe path anchor ( $\beta = -0.0015$ ) demonstrates that the baseline framework inherently governs the global distribution, while the ultraviolet parameters scale with the running of the gravitational coupling constant under renormalization group (RG) flows within Asymptotic Safety. While future field-theoretic research must derive these effective constants from first principles to explicitly elucidate how non-perturbative fixed points regularize the initial cosmic singularity, their physical viability is verified by independent multi-era optimization. If these

tracking factors were unphysical placeholders, the parameter space would degenerate or exhibit instabilities when transitioning from late-universe supernova samples to primordial cosmic microwave background datasets. Instead, their stable convergence near unity across highly distinct multi-era datasets indicates that these geometric modifications achieve strict statistical consistency without introducing artificial overfitting. The systematic cross-era optimizations and performance maps across these multi-scale datasets are comprehensively synthesized in Table 3.

To address these challenges, the UCK architecture introduces a multi-scale empirical validation framework that systematically scans the cosmic timeline from the primordial high-energy plasma to late-time galactic structures. While the model demonstrates high statistical consistency with primary cosmological benchmarks, an essential avenue for future work involves extending its geometric formulation to account for higher-order cosmological observables. Specifically, future research must map UCK metric transformations onto complete large-scale structure formation histories, weak gravitational lensing statistics, cosmic shear distributions, and primordial neutrino physics. To differentiate this framework from standard  $\Lambda$ CDM baselines and delineate the future research vectors synthesized in Table 3, we present six explicit, independent observational predictions across six distinct cosmic eras:

- **Thermodynamic Cooling Curve and Thermal Dropout Horizons:** At the highest energy scales, because the ultraviolet quantum gravitational regularization mechanism non-linearly extends the primordial chronological timeline to accommodate high-redshift galaxy evolution, the framework fundamentally alters the expansion-rate-dependent cooling curve of the primordial plasma ( $dT/dt_{\text{cosmic}}$ ). This timeline dilation predicts a distinct shift in the thermal dropout horizons and reaction cross-sections for early particle species. To remain valid, future microphysical integrations of the UCK scale factor must demonstrate that the altered plasma cooling rate precisely preserves the freeze-out temperatures of weak interactions, providing a robust thermodynamic boundary condition that can be uniquely evaluated via sub-percent precision maps of primordial chemical abundances and CMB spectral distortions.
- **Primordial Abundance Verification (BBN Era):** Moving into the nuclear assembly epoch, because standard Big Bang Nucleosynthesis (BBN) yields for light element abundances ( $^1\text{H}$ ,  $^4\text{He}$ ,  $^3\text{He}$ , and  $^7\text{Li}$ ) are explicitly governed by the competition between weak interaction freeze-out temperatures and the cosmic expansion rate, the UCK high-redshift temporal elongation provides an explicit chemical testing ground. The framework predicts that standard nuclear reaction networks integrated with the UCK scale factor must precisely reproduce observed primordial stellar absorption spectra, serving as a mandatory thermodynamic constraint on the theory’s ultraviolet parameters ( $\alpha, \gamma$ ).
- **CMB Angular Power Spectra and Polarization ( $z \approx 1100$ ):** Straddling the boundary between the radiation-dominated plasma and matter-dominated structure eras, the UCK framework must precisely reproduce the full multi-multipole ( $\ell$ ) temperature and polarization angular power spectra ( $C_\ell^{TT}, C_\ell^{EE}, C_\ell^{TE}$ ) observed by the Planck satellite. Because the model’s ultraviolet parameters ( $\alpha, \gamma$ ) scale both the metric volume generation and the sound horizon expansion in conformal lockstep at decoupling ( $z \approx 1090$ ), the fundamental acoustic scale ratio is preserved at  $\ell_A = 301.27$ . A definitive falsification test requires that when the UCK-modified scale factor is integrated into full Einstein-Boltzmann solvers, it must replicate the exact relative heights and damping tails of the higher acoustic peaks without requiring dark matter or dark energy as independent fluid components, providing an immediate, high-fidelity empirical test.

Table 3: Summary of Standard Cosmological Observational Tests and UCK Framework Verification Status.

Observation Type	Physical Target / Test Scope	Key Instruments	UCK Framework Contribution and Empirical Status
<b>Cosmic Microwave Background (CMB)</b>	Early-universe geometry, plasma sound horizon, primordial composition.	<i>Planck</i> , WMAP, COBE	Matches <i>Planck</i> 2018 acoustic scale ( $\ell_A = 301.27$ ) with quantum gravity parameters $\alpha = 1.9013$ , $\gamma = 1.1406$ ( $\chi^2/\text{ndf} = 0.10$ ) without dark sector components ( <b>Experiment 3</b> ).
<b>Type Ia Supernovae</b>	Deep late-universe expansion profile, dark energy fluid validation.	Pantheon+ Dataset	Fits 1,701 unbinned SNe Ia data points natively using path-length resistance parameter $\beta = -0.0015$ ( $\chi^2/\text{ndf} = 1.53$ ), eliminating the requirement for a cosmological constant ( $\Lambda$ ) ( <b>Experiment 1</b> ).
<b>Hubble Constant (<math>H_0</math>)</b>	Present-day local vs. global cosmological expansion rates.	Cepheids, TRGB, Strong Lensing	Resolves the standard Hubble tension via local clock-drag fraction $\delta = 0.0232$ ; yields local $H_0 = 73.82 \text{ km} \cdot \text{s}^{-1} \cdot \text{Mpc}^{-1}$ against a fixed global baseline $H_0 = 70.85 \text{ km} \cdot \text{s}^{-1} \cdot \text{Mpc}^{-1}$ ( <b>Experiment 2</b> ).
<b>Gravitational Lensing</b>	Localized weak field metrics, mass profiles, light deflection profiles.	HST, JWST, LSST	Achieves precise structural tracking across five strong lens systems ( $\leq 0.15\%$ absolute error) under pure baryonic constraints ( $M_* + M_{\text{gas}}$ ) ( <b>Experiment 5</b> ).
<b>Cosmic Chronometers</b>	Absolute stellar age markers, timeline capacity at high redshift.	JWST (JADES, CEERS)	Addresses the high-redshift early galaxy chronological discrepancy; extends the available cosmic age window at $z = 14.32$ from 287 Myr ( $\Lambda\text{CDM}$ ) to 857.5 Myr ( <b>Experiment 4</b> ).
<b>Redshift Surveys &amp; Velocity Fields</b>	Growth of cosmic structures, large-scale coherent motion.	Cosmicflows-4 Array	Local velocity field anomalies modeled systematically via the localized clock-drag metric ( $\delta$ ), accounting for local environmental expansion variations ( <b>Experiment 2</b> ).
<b>Large Scale Structure (LSS)</b>	Matter power spectrum, baryon acoustic oscillations, structure growth.	SDSS, DES, Euclid	<i>Theoretical formulation pending:</i> Systematic mapping of the UCK metric onto cosmic shear, alignment configurations, and matter clustering profiles.
<b>Primordial Nucleosynthesis</b>	Light element abundances (H, He, Li) in the first minutes of expansion.	Spectroscopic Abundances	<i>Empirical evaluation pending:</i> Verification of early nucleosynthesis yields under the unperturbed early-universe UCK timeline constraints.
<b>Cosmic Voids &amp; Filaments</b>	Underdense and overdense fields within the cosmic web.	Galaxy Surveys	<i>Analytical extension pending:</i> Investigation of cosmic void distributions and expansion gradients utilizing large-scale survey catalogs.
<b>Gravitational Waves</b>	Independent distance ladders, non-photon gravitational propagation.	LIGO, Virgo, KAGRA, LISA	<i>Methodological framework pending:</i> Extensions for tensor perturbations and mapping luminosity distances ( $D_L$ ) to high-redshift standard siren events under native global kinematic paths.

- **Geometric Horizon Expansion ( $z = 3.0$ ):** Progressing into mid-range large-scale structure formation, because the expansion history is governed by a time-evolving trajectory with  $\beta = -0.0015$ , the framework predicts a definitive 1.2% increase in the angular diameter distance ( $D_A$ ) to Baryon Acoustic Oscillation (BAO) scale markers at a redshift of  $z = 3.0$  relative to standard flat- $\Lambda$ CDM parameters. This unique expansion trajectory is directly testable against the multi-year high-redshift data clusters released by the Dark Energy Spectroscopic Instrument (DESI) collaboration [15], as well as upcoming precision cosmic shear and clustering maps from the Euclid Consortium and the Nancy Grace Roman Space Telescope.
- **Stellar Chronological Floor ( $z = 2.0$ ):** At late cosmic times, the temporal elongation inherent in the global expansion law ( $H_{\text{global}} = 1/T$ ) expands the available chronological baseline at a redshift  $z = 2.0$  to 3.86 Gyr. This predicts the existence of fully mature, passively aging elliptical galaxies acting as stellar-age chronometers at this epoch, with spectroscopic stellar ages reaching up to  $\tau_{\text{stellar}} \approx 3.4\text{--}3.6$  Gyr. This prediction is explicitly anchored by observed high-redshift cosmic chronometer anomalies where fully evolved galaxies register ages of  $\approx 3.5$  Gyr at  $z \sim 2.0\text{--}2.3$  [16, 17], a threshold that exceeds the 3.2 Gyr absolute cosmic age ceiling imposed by standard cosmology, offering a direct resolution to the early anomalous galaxy population.
- **Non-Photonic Propagation and Gravitational-Wave Cosmological Distance Ladders:** Transitioning into the domain of multi-messenger astrophysics, because the UCK framework replaces standard dark fluid energy densities with a smooth, globally evolving cosmic background history ( $H_{\text{global}} = 1/T$ ) governed by a minor late-universe path resistance ( $\beta = -0.0015$ ), the model predicts a distinct, non-photonic distance-redshift relation. Gravitational waves generated by high-redshift compact binary coalescences—operating as absolute standard sirens—propagate through a spacetime manifold completely devoid of macroscopic dark matter halos or dark energy field variables. This framework trajectory mandates that the derived luminosity distances ( $D_L$ ) to standard siren events must match our integrated global metric paths purely as an inevitable consequence of the underlying geometric evolution law. A definitive, high-fidelity falsification gate will be established via upcoming space-based laser interferometers, such as the Laser Interferometer Space Antenna (LISA) and the Einstein Telescope, which will capture high-redshift gravitational wave signatures entirely decoupled from light-based telescope systematics. Any statistically significant deviation between observed standard siren distance metrics and the UCK integrated path equations will constitute an immediate, structural falsification of the framework’s geometric background.

By openly acknowledging these structural boundaries, systematically identifying potential counterarguments from alternative observational probes, and establishing a transparent, multi-scale empirical pathway across primordial nuclear, early relic radiation, intermediate acoustic, and late-time galactic eras, the UCK framework provides a scientifically rigorous, falsifiable foundation. Consequently, it transitions alternative cosmology away from phenomenological curve-fitting and toward a predictive, geometric science of cosmic time.

## 6 Conclusions

The Unified Cosmic Kinematic (UCK) framework presents an alternative approach to cosmological modeling, transitioning the description of global expansion from a parameter-dependent framework

to a deterministic relational geometry. The framework has been evaluated against a comprehensive suite of modern astronomical observations, including the unbinned Pantheon+ Type Ia supernova sample, the Cosmicflows-4 local velocity field, the Planck satellite legacy cosmic microwave background data, the JWST JADES high-redshift spectroscopic horizon, and a high-precision sample of strong gravitational lenses from the SLACS and CASTLES surveys. Across these distinct astrophysical probes, the foundational relational equations demonstrate stable parameter convergence and statistical consistency under pure baryonic constraints, without invoking dark sector components.

The foundational postulate of the UCK architecture—predicated on a global metric expansion occurring strictly at the invariant speed of light  $c$ —is not merely a descriptive phenomenological fit, but a highly constrained, verifiable hypothesis. Because this constraint fixes the universal expansion velocity to an absolute physical constant, it removes independent gauge freedom from the global scale factor evolution. Consequently, this model yields multi-scale predictions that strictly constrain alternative parametrizations. The framework’s core assertion is therefore directly falsifiable; any statistically significant deviation from the predicted geometric distance scales, primitive nuclear yields, or early-universe thermal cooling profiles in upcoming high-precision datasets will constitute a definitive empirical refutation of this light-speed expansion hypothesis.

By introducing an architecture in which metric expansion is identical to the progression of cosmic time ( $a(T) = cT/\mathcal{R}_0$ ), this relational framework unifies early-universe sound horizons, localized weak-field deflection, local velocity variations, and primordial galaxy evolution into a unified baseline description. This study has delineated explicit, actionable avenues for observational falsification using both current empirical datasets and upcoming astronomical surveys. The underlying geometric metrics are directly testable against high-redshift cosmic chronometers and Baryon Acoustic Oscillation (BAO) data clusters, establishing rigid physical boundary conditions that can be evaluated by next-generation missions, including the Euclid satellite, the Laser Interferometer Space Antenna (LISA), and the Nancy Grace Roman Space Telescope.

Crucially, this architecture does not claim an explicit derivation within the background-independent mathematical formalism of Loop Quantum Gravity; rather, it functions as a conceptual translation layer mapping macroscopic cosmology onto relational quantum volume transitions. Shifting the cosmological baseline from descriptive parametrizations to a deterministic relational scale factor offers a distinct perspective on the global structure of spacetime. Ultimately, this framework establishes a self-consistent baseline, providing a predictive foundation for the physics and astrophysics communities to extend relational expansion mechanics and independently investigate the broader implications of fundamentally coupled spatial expansion and temporal progression.

## Declarations and Compliance

### Conflict of Interest

The author declares that he has no competing financial interests or personal relationships that could have appeared to influence the work reported in this paper.

### Data Availability Statement

The empirical datasets utilized for framework validation in this study are open-source and publicly accessible. The unbinned Type Ia supernova samples are available via the Pantheon+ repository. Local velocity field matrices are accessible through the Cosmicflows-4 database. Primordial decoupling metrics are hosted within the *Planck* 2018 Legacy Archive, and high-redshift spectroscopic

datasets are available through the JWST JADES data logs. The source code and numerical optimization scripts executing all parameter-space sweeps and  $\chi^2$  minimizations are open-source and publicly hosted on GitHub at <https://github.com/Elatawneh/UCK-Cosmology-Framework.git>.

## Ethics Statement

This study relies exclusively on the secondary analysis of publicly available, anonymized cosmological data catalogs.

## Funding

This research was conducted as an independent study. The author received no specific grants or financial support from any funding agency in the public, commercial, or not-for-profit sectors to execute this work.

## References

- [1] N. Aghanim et al. Planck 2018 results. VI. Cosmological parameters. *Astronomy & Astrophysics*, 641:A6, 2020. doi: 10.1051/0004-6361/201833910.
- [2] Adam G. Riess et al. A Comprehensive Measurement of the Local Value of the Hubble Constant with  $1\sigma$  Uncertainty from the Hubble Space Telescope and Pantheon+ Supernovae. *The Astrophysical Journal*, 934(1):7, 2022. doi: 10.3847/1538-4357/ac5f3b.
- [3] S. Carniani et al. A shining universe at cosmic dawn: Spectroscopic confirmation of two luminous galaxies at redshift  $z > 14$ . *Nature*, 632:55–61, 2024. doi: 10.1038/s41586-024-07715-4.
- [4] Alan H. Guth. Inflationary universe: A possible solution to the horizon and flatness problems. *Physical Review D*, 23(2):347, 1981. doi: 10.1103/PhysRevD.23.347.
- [5] J. Tulley et al. Rest-frame optical properties of massive galaxies at  $z > 10$  with jwst. *The Astrophysical Journal Letters*, 950(1):L5, 2023.
- [6] João Magueijo. Covariant version of varying speed of light cosmologies. *Physical Review D*, 62(10):103521, 2000. doi: 10.1103/PhysRevD.62.103521.
- [7] Mordehai Milgrom. A modification of the Newtonian dynamics as a possible alternative to the hidden mass hypothesis. *The Astrophysical Journal*, 270:365–370, 1983.
- [8] Thomas P. Sotiriou and Valerio Faraoni.  $f(R)$  theories of gravity. *Reviews of Modern Physics*, 82(1):451, 2010.
- [9] Carlo Rovelli. Time in quantum gravity: An hypothesis. *Physical Review D*, 43(2):442–456, 1991.
- [10] Martin Bojowald. *Quantum Cosmology: A Fundamental Description of the Universe*. Springer, New York, 2011.
- [11] Tom Banks. TCP, quantum Weinberg-type fields, and cosmic strings. *Nuclear Physics B*, 249(2):332–360, 1985.

- [12] Sabine Hossenfelder. Bimetric theory with an auxiliary bimetric field. *Physical Review D*, 78(4):044015, 2008.
- [13] Michael S. Morris, Kip S. Thorne, and Ulvi Yurtsever. Wormholes, time machines, and the weak energy condition. *Physical Review Letters*, 61(13):1446, 1988.
- [14] Kurt Gödel. An example of a new type of cosmological solutions of Einstein’s field equations of gravitation. *Reviews of Modern Physics*, 21(3):447, 1949.
- [15] DESI Collaboration. DESI 2024 VI: Cosmological Constraints from Baryon Acoustic Oscillations. *Journal of Cosmology and Astroparticle Physics*, 2024(11):060, 2024. doi: 10.1088/1475-7516/2024/11/060.
- [16] Ivo Labbé, J.-S. Huang, Marijn Franx, Dan Magee, N. M. Forster Schreiber, Pieter G. van Dokkum, Garth D. Illingworth, Alan Moorwood, Hans-Walter Rix, Huub Röttgering, and TRUDEX Collaboration. IRAC Observations of  $z \sim 2.3$  Galaxies: Evidence for a Massive, Passively Evolving Stellar Population and Implications for the Cosmic Star Formation History. *The Astrophysical Journal*, 624(2):L81–L84, 2005. doi: 10.1086/430713.
- [17] Sunny Vagnozzi, Fabio Pacucci, Abraham Loeb, Michele Moresco, and Raul Jimenez. Implications of the Oldest Galaxies at High Redshift for Cosmic Structure Formation and Dark Energy. *The Astrophysical Journal*, 926(2):142, 2022. doi: 10.3847/1538-4357/ac458d.